



Optimization of reactive distillation processes with simulated annealing

M. F. Cardoso, R. L. Salcedo*, S. Feyo de Azevedo, D. Barbosa

Departamento de Engenharia Química, Faculdade de Engenharia da Universidade do Porto, Rua dos Bragas, 4099 Porto, Portugal

Received 6 August 1999; accepted 4 April 2000

Abstract

A simulated annealing-based algorithm (MSIMPISA) suitable for the optimization of mixed integer non-linear programming (MINLP) problems was applied to the synthesis of a non-equilibrium reactive distillation column. A simulation model based on an extension of conventional distillation is proposed for the simulation step of the optimization problem. In the case of ideal vapor–liquid equilibrium, the simulation results are similar to those obtained by Ciric and Gu (1994, *AIChE Journal*, 40(9), 1479) using the GAMS environment and to those obtained with the AspenPlus modular simulator. The optimization results are also similar to those previously reported and similar to those using an adaptive random search algorithm (MSGGA). The optimizations were also performed with non-ideal vapor–liquid equilibrium, considering either distributed feed and reaction trays or single feed and reaction tray. The results show that the optimized objective function values are very similar, and mostly independent of the number of trays and of the reaction distribution. It is shown that the proposed simulation/optimization equation-oriented environments are capable of providing optimized solutions which are close to the global optimum, and reveal its adequacy for the optimization of reactive distillation problems encountered in chemical engineering practice. © 2000 Elsevier Science Ltd. All rights reserved.

Keywords: Simulated annealing; Reactive distillation; Simulation; Optimization

1. Introduction

Reactive distillation columns can be attractive whenever conversions are limited by unfavorable reaction equilibrium and when selectivity can be increased by allowing simultaneous reaction and separation in the same processing unit. These are the two main advantages of reactive distillation over more conventional alternatives (Barbosa & Doherty, 1988a,b; Okasinski & Doherty, 1998), whereby the total annualized production cost can be decreased by an order of magnitude (Doherty & Buzad, 1992).

Reactive distillation processes have received attention since the beginning of the century, when the first proposal for the use of a distillation column as a reactor was considered. In the early 1920s a number of patents were registered for carrying out esterification reactions in distillation columns (Backhaus, 1921a–c 1922a–e 1923a,b). Most of the work preceding 1970 refer to experimental

studies in reactive distillation. Afterwards, rigorous mathematical models for computer simulation began to be developed. These are essentially extensions of methods available for conventional distillation (Suzuki, Yagi, Kamatsu & Hirata, 1971; Hunek, Foldes & Sawinsky, 1979; Murthy, 1984; Chang & Seader, 1988; Doherty & Buzad, 1992).

Most of the studies in reactive distillation are simulation studies, viz. the resulting composition profiles are determined after specification of feed composition and quality, column pressure, reflux or reboiler ratio, total number of stages, feed plate location and liquid-phase volumes on each stage. There are several simulation algorithms available (Buzad & Doherty, 1995), some implemented in commercial simulators, such as Aspen-Plus (Venkataraman, Chan & Boston, 1990). Abufares and Douglas (1995) developed a dynamic mathematical model for a methyl tertiary butyl ether (MTBE) catalytic distillation process, which was implemented in the dynamic simulator SpeedUp. Recently, Huss, Chen, Malone and Doherty (1999) proposed a general framework based on conceptual design for solving both equilibrium and rate-based reactive distillation processes. Also,

* Corresponding author. Fax: 351-2-2000808.

E-mail address: rsalcedo@fe.up.pt (R. L. Salcedo).

Schenk, Gani, Bogle and Pistikopoulos (1999) have defined a general modeling framework that allows both rate-based and equilibrium-based models, steady state or dynamic, to be formulated and solved. Jimoh, Arellano-Garcia, Bock and Wozny (1999) have experimentally validated their steady-state and dynamic model for reactive distillation using a pilot-scale column and investigated the transesterification of methyl myristate with isopropanol to methanol and isopropyl myristate.

In the simulation of a distillation column the resulting separation is evaluated for a specified column, while in a design problem the desired separation is specified and the column parameters are then evaluated (Buzad & Doherty, 1995). While it has been relatively easy to extend simulation methods developed for non-reactive distillation, it has not been easy to extend non-reactive distillation design techniques to reactive distillation columns.

There are several reasons for the difficulty in developing methods for the design of reactive distillation processes, as referred by Ciric and Gu (1994). In conventional distillation design, the major design variables are the number of trays in the column, the feed tray location and the reflux ratio. It is usually reasonable to assume constant molar flow rate in each column section, and that each feed stream is introduced in a single tray. In opposition, in reactive distillation processes the molar flow rates can only be set constant if the following conditions are also verified: heat of reaction negligible and the total number of moles constant. The liquid holdup on each tray cannot be ignored, even for steady-state operation, since it is here that reactions take place and it is this volume that determines the extent of the reactions.

Barbosa and Doherty (1988a,b), Ciric and Gu (1994), Buzad and Doherty (1995), Pekkanen (1995), Okasinski and Doherty (1998) and Huss et al. (1999) are some of the researchers who developed methods for the design of reactive distillation columns.

Barbosa and Doherty (1988a,b) developed techniques based on methods applicable to the design of conventional distillation columns. However, these techniques were developed for systems near chemical equilibrium, with constant molar flow and which involve a single reaction. When any one of these assumptions is violated, the method is no longer valid.

Ciric and Gu (1994) proposed an interesting technique for the design of reactive distillation columns, by formulating a synthesis problem which can be applied to more generic situations, when there is more than one chemical reaction, or when reactive equilibrium or constant molar flow cannot be assumed. With their column model they have built a mixed integer non-linear programming (MINLP) problem. The solution of this problem yields the optimum number of trays, the optimal feed tray location(s) and composition(s), and the composition profiles within the column. These authors solved the

MINLP problem using a generalized Benders decomposition algorithm (Geoffrion, 1972).

Buzad and Doherty (1995) developed a procedure which determines the optimum value for the total amount of liquid holdup for a fixed product composition. The procedure is a fixed point method which divides the composition space into regions of feasibility, and is presented as an alternative to methods developed for reactive distillation columns operating close to reaction equilibrium conditions. The procedure was developed for distillation processes with three components where reactions such as $2C \rightleftharpoons A + B$ occur.

Pekkanen (1995) presents a design algorithm for a 'local optimization' approach for reactive distillation. This approach is characterized as a 'stage by stage specification', where the design procedure starts from both column ends and design specifications are made at each stage as the calculation progresses. The column is thus not optimized as a whole since not all the parameters are simultaneously varied.

Okasinski and Doherty (1998) have extended the fixed point design method for systems with isomolar or non-isomolar liquid-phase reaction, non-ideal vapor-liquid equilibrium and allowing for a distribution of liquid holdups on the reactive stages.

Huss et al. (1999) give emphasis to conceptual column design through geometric methods, and have shown that equilibrium reactive designs can be the starting point for rate-based designs.

In this work, we propose an integrated approach to the simulation/optimization of reactive distillation columns, by adopting the MINLP column model of Ciric and Gu (1994). The simulation model is based on an extension of conventional distillation columns and the optimization is performed by a simulated annealing-based MINLP algorithm (the MSIMPISA algorithm of Cardoso, 1998). Results are also compared with those obtained using an adaptive random search algorithm (the MSGA algorithm of Salcedo, 1992). The proposed method can be applied to single or multiple reactions, ideal or non-ideal vapor-liquid equilibrium and distributed or single-staged reaction zones.

2. Simulated annealing and the MSIMPISA algorithm

Simulated annealing is a well-established technique for the optimization of combinatorial problems, i.e. for the optimization of large-scale functions that may assume several distinct discrete configurations (Metropolis, Rosenbluth, Rosenbluth, Teller & Teller, 1953; Kirkpatrick, Gellatt & Vecchi, 1983). It may also be used for continuous (NLP) or mixed-integer (MINLP) problems. For a review of the available algorithms, the reader should refer to the available literature (Cardoso, Salcedo & Azevedo, 1994, 1996).

Briefly, the Metropolis algorithm simulates the physical process of annealing, i.e. melting a solid by increasing its temperature, followed by slow cooling and crystallization into a minimum free energy state. From an optimization point of view, simulated annealing explores the key feature of the physical annealing process of generating transitions to higher energy states, applying to the new states an acceptance/rejection probability criterion which should naturally become more and more stringent with the progress of the optimization. Thus, simulated annealing may be viewed as a randomization device that allows some wrong-way movements during the course of the optimization, through an adaptive acceptance/rejection criterion (Schoen, 1991). It is recognized that these are powerful techniques which might help in the location of near-optimum solutions, despite the drawback that they may not be rigorous (except in an asymptotic way) and may be computationally expensive (Grossmann & Daichendt, 1994).

The SIMPSA solver (Cardoso et al., 1996) is a simulated annealing-based algorithm that was developed for solving constrained NLP problems. It is built on a scheme proposed by Press and Teukolsky (1991) for unconstrained continuous optimization, and combines the simplex method of Nelder and Mead (1965) with simulated annealing. The role of the non-linear simplex is to generate continuous system configurations, while the role of simulated annealing is to allow for wrong-way movements, simultaneously providing (asymptotic) convergence to the global optimum. The algorithm showed good robustness, viz. good insensitivity to the starting point, and reliability in attaining the global optimum, for a number of difficult NLP problems described in the literature (Cardoso et al., 1996). It may also be used with a faster non-equilibrium variant of simulated annealing (Cardoso, Salcedo & Azevedo, 1994).

The MSIMPSA algorithm (Cardoso et al., 1997) was developed as an extension of the SIMPSA solver to deal with MINLP problems. The continuous non-linear solver is used in an inner loop to update the continuous parameters, while the Metropolis algorithm is used in an outer loop to update the complete set of decision variables. The stochastically generating scheme proposed by Dolan, Cummings and Levan (1989) is employed each time a different set of discrete variables is needed, whereby a first random number chooses the discrete variable to be changed and a second one chooses if the change is to be upwards or downwards by one unit. The MSIMPSA algorithm is simple to use, since it neither requires the preliminary identification of integer candidates for the global optimum nor the identification of feasible or good starting points. It was tested with several difficult MINLP functions published in the literature, showing a good robustness in attaining the global optimum. The MSIMPSA algorithm has a wide applicability, since it is applicable not only to MINLP problems, but also to

NLP and combinatorial problems. When applied to NLP problems, it performs as the SIMPSA algorithm (Cardoso et al., 1996) and when applied to combinatorial problems it performs as the original Metropolis algorithm (Cardoso et al., 1994).

3. Synthesis of a reactive distillation column for the production of ethylene glycol

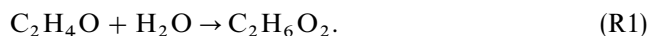
3.1. Problem definition

The synthesis problem for designing a reactive distillation column is stated by Ciric and Gu (1994) as follows. Given:

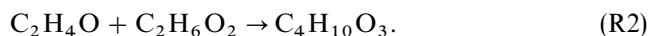
- a set of chemical species $i = 1, \dots, I$,
- a set of desired products and production rate,
- a set of chemical reactions $j = 1, \dots, R$, the stoichiometric coefficients for all species, v_{ij} , and rate expressions $r_j = f(x_i, T)$,
- the enthalpy of vaporization and vapor–liquid equilibrium data,
- the feed streams composition,
- the cost parameters,

the goal is to determine the optimal number of trays, holdup per tray, reflux ratio, condenser and reboiler duties and feed tray locations. Fig. 1 shows a schematic diagram of the process.

Ethylene glycol ($C_2H_6O_2$) is produced from the reaction of ethylene oxide (C_2H_4O) and water:



However, the ethylene glycol produced can further react with ethylene oxide to produce the unwanted by-product diethylene glycol ($C_4H_{10}O_3$):



Both reactions are highly exothermic and occur at moderate temperatures, allowing production via a reactive distillation column.

According to Ciric and Gu (1994) there are two reasons for producing ethylene glycol via reactive distillation. Firstly, the large difference in volatilities between ethylene oxide and ethylene glycol will lead to a rapid separation of these two components in the column, improving the overall selectivity. Secondly, part of the heat required for the separation is obtained from the heat of reaction, which allows the reduction of energy costs.

Data for this problem can be found in Appendix A — Table 6 (reaction data), Table 7 (vapor–liquid equilibrium constants, ideal VLE), Table 8 (cost data) and Table 9 (thermodynamic data, non-ideal VLE). The

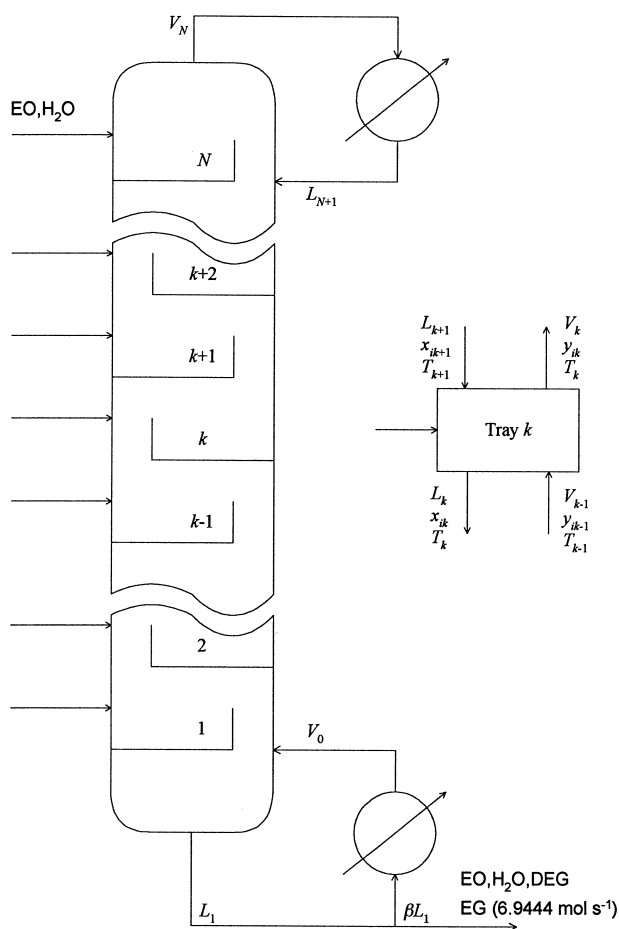


Fig. 1. Schematic diagram of a reactive distillation column for the production of ethylene glycol.

enthalpy of vaporization of the mixture is assumed to be constant all over the column with the value of $40 \times 10^3 \text{ J mol}^{-1}$ (Ciric, 1995). The mathematical formulation of this problem as formulated by Ciric and Gu (1994) is completely described in Appendix B. The constant C_D used for evaluating the column diameter (Eq. (B.24)) has the value 0.01331 (dimensionless).

The objective function is the minimization of the total annualized cost which is composed of two basic terms: annual operating costs and the annualized investment. The raw material, steam and cooling water set the annual operating costs. The costs of the column shell, trays, reboiler and condenser correspond to the annualized investment. To evaluate the objective function, the operating conditions determined by the column simulation for each decision vector have to be known.

3.1.1. Constraints

Ciric (1995) has set as 1000 kmol h^{-1} the maximum value for the vapor and liquid flow rates, 14.16 m^3 for the

maximum value of the liquid holdup, and 20 for the maximum number of trays. Although these limits are not strictly necessary for the optimization step, they were initially enforced for comparing our results with those from Ciric and Gu (1994). These constraints are

$$V_k \leq F_{\max}, \quad k = 1, \dots, N,$$

$$L_k \leq F_{\max}, \quad k = 1, \dots, N,$$

$$\sum_{i=1}^c F_{ik} \leq F_{\max}, \quad k = 1, \dots, N,$$

$$W_k \leq W_{\max}, \quad k = 1, \dots, N,$$

as well as the maximum number of trays, N_{\max} . The feed to the distillation column in each tray is composed of one feed stream of ethylene oxide and one feed stream of water. Obviously, some of these feeds may have a null value. This problem can be considered as a fairly large highly non-linear non-convex problem (function of N_{\max}), since the material balances contain bi and trilinear terms and the reaction terms, the vapor-liquid equilibrium evaluation and the objective function are highly non-linear.

For the optimization problem under study, there are $(3N_{\max} + 1)$ decision variables. One is integer corresponding to the maximum number of trays, N_{\max} , and $3N_{\max}$ decision variables are continuous: the boil-up fraction, β , N_{\max} feed flow rates corresponding to one of the components, ethylene oxide or water, $N_{\max} - 1$ feed flow rates corresponding to the other component (all but the feed flow rate into the first tray next to the reboiler), and N_{\max} liquid holdups. For a maximum number of 20 trays there are 341 variables and 61 degrees of freedom, where one is integer. The integer variable can be represented by six binary variables according to a binary expansion (Cardoso et al., 1997), since with the binary expansion larger variations of the original discrete variable are allowed at each step of the optimization process.

For the simulation of a column with N_{\max} trays, all the $3N_{\max}$ continuous variables are required; however, for a column with N trays, where $N < N_{\max}$, only $3N$ continuous variables are involved while the other $3(N_{\max} - N)$ are simply ignored.

3.2. Simulation algorithm

The simulation of reactive distillation processes involves the simultaneous solution of material and energy balances and stoichiometric relationships, and this corresponds to the solution of a considerable large set of non-linear equations. The calculation procedures reported for solving sets of non-linear equations can be divided broadly into four categories (Chang & Seader, 1988; Venkataraman et al., 1990; Biegler,

Grossmann & Westerberg, 1997; Lee & Dudukovic, 1998):

- (i) methods using equation decomposition (or tearing/partitioning);
- (ii) relaxation techniques;
- (iii) methods incorporating Newton or quasi-Newton algorithms;
- (iv) homotopy-continuation methods.

Decomposition methods allow the identification of blocks which need the simultaneous solution and blocks which can be solved sequentially. For example, Ledet and Himmelbleau (1970) propose a method that identifies a minimum set of recycle variables, which may then be used with direct substitution. These methods are fast and efficient in what concerns the use of computer storage space. However, when differences in boiling point values between components are large, when kinetics are complex, or when liquid solutions are highly non-ideal, these direct methods suffer from poor convergence characteristics.

With relaxation techniques, the liquid-phase compositions are computed based on non-steady-state material balances (Bastos, 1987), which in subsequent iterations proceed towards the steady-state solution. Relaxation techniques are reliable but can be slow specially as the solution is approached (Bastos, 1987; Chang & Seader, 1988; Venkataraman et al., 1990).

Newton or quasi-Newton methods converge quickly from suitable starting guesses (Murthy, 1984; Chang & Seader, 1988). When the starting point is far from the solution, these methods can converge to impossible physical conditions or may not converge at all. Bastos (1987) has developed an algorithm for the simulation of conventional distillation columns that makes use of a modified Newton–Raphson method. As a first step the algorithm applies a relaxation technique to improve the starting guess for the composition profile and flow rates in the column, which are needed by the Newton–Raphson method.

Homotopy-continuation methods have the advantage of forcing the desired solution by tracking a homotopy curve regardless of the choice of the initial estimates. Lee and Dudukovic 1998 have found these to be superior to Newton-based methods for solving the non-linear system of equations arising in reactive distillation, despite a longer computational burden.

In this work, we propose a procedure for the simulation of reactive distillation columns based on the method developed by Bastos (1987) for conventional distillation columns (see Appendix C). Table 1 shows the variables' identification, both calculated and specified by the simulation algorithm.

3.2.1. General structure of the simulation problem

For the reactive distillation column specified as above, we propose a simulation model based on the

Table 1
Variables calculated and specified — simulation algorithm

Variable	Number	Specified	Calculated
Number of trays	1	1	
Compositions			
Liquid	$C(N + 1)$		$C(N + 1)$
Distillate	C		C
Flow rates			
Liquid	$N + 1$		$N + 1$
Vapor	$N + 1$		$N + 1$
Distillate	1	1	
Bottom components	C	1	$C - 1$
Feeds	NN_F	$NN_F - 1$	1
Column temperatures	N	P	N
Boil-up fraction	1	1	
Liquid holdups	N	N	
Duties			
Condenser	1		1
Reboiler	1		1
Extent of reactions	NR		NR
Vapor–liquid equilibrium constants	NC		NC
Column dimensions			
Diameter	1		1
Height	1		1
Total	$N(N_F + 2C + R + 4) + 3C + 9$	$N(N_F + 1) + 3$	$N(2C + R + 3) + 3C + 6$

following steps:

- (i) An initial estimate of the molar feed flow rate not specified by the decision vector, viz. a torn (recycle) variable, is specified. We have chosen F_{21} as the torn variable, although other recycle variables may equally work. This torn variable was found to be appropriate from an information flow point of view, and need not be a true recycle variable (from a material flow point of view).
- (ii) An initial estimate of the composition profile in the column is next obtained.
- (iii) This estimate is improved by a relaxation method.
- (iv) The material balance equations are then solved with the Newton–Raphson method, and a new composition profile is computed.
- (v) The torn variable is re-evaluated and the equations describing the reactive distillation process are again solved (Fig. 2).
- (vi) The algorithm ends up when the global material balance to the column is verified (after convergence on the torn variable) or when a non-plausible column is obtained.

The simulation is aborted when convergence on the torn variable is obtained but not on the global material balance, or when the Newton–Raphson method exceeds a pre-specified maximum number of iterations. When one of these situations is verified, the column is infeasible and the objective function value is simply penalized with a large constant value. This simple penalizing scheme is possible due to the stochastic nature of the optimization algorithms employed in the present work.

The simulation algorithm was written in Fortran 77, and all runs were performed with double precision on a HP 730 Workstation, running compiler optimized Fortran 77 code. The average time spent in each simulation varied from 0.1 s for a two-tray column to about 1.5 s for a column with 20 trays.

3.2.2. Details on initialization

The starting guess of the torn variable F_{21} should be large enough to accommodate the desired production rate, considering that conversion is not complete. When the simulation starts, this variable is estimated such that the sum of all the feed flow rates of this component is at least 50% larger than the specified production flow rate of ethylene glycol. This value was set by taking into account several items: the stoichiometry of the ethylene glycol production reaction (reaction (R1)), the existence of a secondary reaction that produces diethylene glycol from ethylene glycol (reaction (R2)); and that not all the water fed to the column reacts, some exiting the column with the products.

For the subsequent step of the simulation of a reactive or non-reactive distillation column, a starting guess for the composition profile is also necessary. For non-reactive distillation the guessed initial composition profile is generally based on feed compositions, considering the same liquid composition all over the column (Bastos, 1987):

$$x_{ij} = \frac{\sum_{j=1}^N F_{ij}}{\sum_{i=1}^C \sum_{j=1}^N F_{ij}}, \quad i = 1, \dots, C; j = 1, \dots, N. \quad (1)$$

This procedure is sometimes used also with reactive distillation processes (Murthy, 1984). However, the starting profile can be too far from the correct one, driving the simulation to impossible physical conditions or to non-convergence of the iterative process. This can occur, for instance, when one of the feed species corresponds to a reactant with a high consumption rate.

Venkataraman et al. (1990) initialize the column composition profile by flashing the feed at the average column pressure, taking the different reactions into account. Schenk et al. (1999) solve firstly a simple equilibrium model, and next more complex simulations using as initial guesses the results from the previous simulations. The same approach is adopted by Huss et al. (1999) in

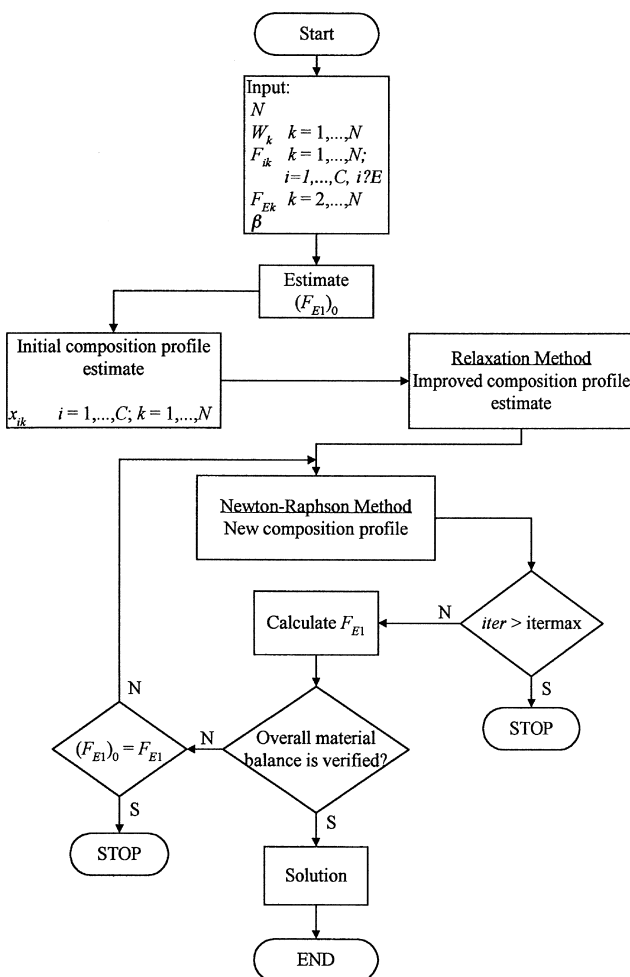


Fig. 2. Simulation algorithm.

their conceptual design of non-equilibrium reactive models. Lee and Dudukovic (1998) assume the liquid phase to be an ideal solution and the starting temperature profile to be linear.

Most of the authors, however, do not refer any method to generate the initial conditions necessary to start the iterative process. Venkataraman et al. (1990), who incorporated their algorithm for the simulation of reactive distillation columns in the AspenPlus simulator, refer that a correct initialization by the user can improve the success of the starting point.

An algorithm for the initialization of the composition profile for the case study was developed taking into account the two reactions and the specified product flow rate. From the stoichiometry of the reactions, the following relations are obtained:

$$P_1 = \sum_{k=1}^N F_{1k} - P_3 - 2P_4, \quad (2)$$

$$P_2 = \sum_{k=1}^N F_{2k} - P_3 - P_4. \quad (3)$$

The P_4 flow rate is estimated with Eq. (2) if the total ethylene oxide feed flow rate is less than the total water feed flow rate, otherwise it is estimated with Eq. (3). This estimate is performed by supposing that the reactant with the lower total feed flow rate has a consumption rate near 100%. The other reactant product flow rate is estimated with the remainder equation. The composition in the tray next to the reboiler and the global extent of reactions (R1) and (R2) can now be computed with the estimates of all product flow rates, P_1 – P_4 .

The initial composition profile is estimated based on the following assumptions:

- (i) The extent of reactions (R1) and (R2) is the same in all trays with liquid holdup, and null in all the other trays.
- (ii) The starting guess for the composition of the liquid phase on the last tray, N , is 95% of component 2 and 5% of component 3.
- (iii) The composition of component 1 on tray N is re-evaluated if liquid holdup for reaction exists. This composition value must be correctly estimated because if it is null, then the reaction term is also null giving rise to infeasible columns. The correction of this composition is performed taking into account the extension value for reaction (R1):

$$\xi_{1N} = W_N k r_{1N} x_{1N} x_{2N}, \quad (4)$$

where W_N is the liquid holdup, $k r_{1N}$ is the reaction constant, and x_{1N} and x_{2N} are the composition of components 1 and 2, in tray N . The composition values for all components are then normalized such that the stoichiometric equation for tray N is obeyed.

This normalization is a common feature of algorithms employed to solve distillation models (Lee & Dudukovic, 1998).

- (iv) For each one of the other trays, with the estimated compositions of the top and bottom trays, the compositions of components 2–4 are computed using linear interpolation, and the composition of component 1 is set null for all trays. If on tray k there is liquid holdup for reaction, the composition of component 1 is recalculated using the procedure for tray N .

With the starting guess for the composition profile, the temperature profile can be computed, as described below, as well as all the other variables of the process.

It should be noted that it is not beneficial to use the previous composition and temperature profiles as the initial point for subsequent iterations, for two reasons: the optimization algorithm may produce at each iteration a completely different number of stages, viz. N does not change sequentially; and the simplex moves, even at each fixed value for N , may produce a distributed feed which is widely different in composition and location. Thus, with the MSIMPISA or MSGA algorithms, it is also not beneficial to start the optimization from a single-tray column.

3.2.3. Temperature profile

The temperature on each tray is computed with the corresponding stoichiometric vapor phase (Eq. (A.12)). The solution of this equation is obtained with the Newton–Raphson method.

3.2.4. Liquid and vapor molar flow rates

The liquid molar flow rate off the first tray is computed with the reboiler material balance for the species corresponding to the specified product (Eq. (B.14)). The vapor flow rate into the first tray, V_0 , is the L_1 fraction vaporized in the reboiler (Eq. (B.19)). Knowing V_0 , the vapor flow rates off all the trays of the column are recursively computed from stage 1 to stage N , using the energy balance over each tray (Eq. (B.13)).

The liquid molar flow rates off each tray of the column are recursively computed from stage N to stage 2, using the global material balance over each tray (Eqs. (B.9) and (B.10)). The liquid molar flow rate into the top tray, L_{N+1} is computed with Eq. (B.16).

3.2.5. Relaxation method

The use of the Newton–Raphson method requires a suitable starting guess for the composition profile. The initial starting guess for the composition profile is subsequently improved by the application of a relaxation method during a pre-specified number of iterations. The relaxation method used is described in Appendix C, and is based on a method described by Bastos (1987) for

non-reactive systems. The extension to reactive systems can be seen, for example, in Murthy (1984).

3.2.6. The Newton–Raphson method

The Newton–Raphson algorithm is used to compute the composition profile by solving the material balance. The application of this method was based on the algorithm proposed by Bastos (1987), but considering that the chemical reaction may be distributed over several column trays, such as described in Appendix C. With non-ideal VLE, it was also considered that the reaction might be circumscribed to a single tray (Okasinski & Doherty, 1998).

As the composition of component 1 in the liquid phase is near zero, the application of the relaxation method to this component would produce large errors, not only in this composition but also in the composition of the other components. Since a reasonable estimate of the composition of component 1 is needed in the trays having liquid holdup, the procedure adopted is similar to that used in the initialization of the composition profile, which requires the reaction extension in each tray. The extension values for the two reactions were set equal to the values previously obtained in the initialization of the column composition profile.

The composition values obtained in the liquid phase are then normalized. With the composition profile, the temperature profile along the column and all the other operating variables are calculated (except the reaction rates which are set constant during the application of the relaxation method). The maximum number of iterations was set at 20, after a preliminary study.

The Newton–Raphson method can also be solved for component molar flows, instead of molar fractions. However, similar numerical problems may occur, since component flows may be very small and become negative. For example, with the data of Ciric and Gu (1994) and the MSIMPSA algorithm, while molar fractions vary from 1.3×10^{-11} to 7.7×10^{-5} , the corresponding component molar flows vary from 3.5×10^{-9} to 2.1×10^{-2} . Also, molar fractions are easier to normalize.

3.2.7. Convergence criteria

The simulation ends up with a feasible distillation column when the global material balance of all components is obeyed. If convergence on the recycle variable is obtained without convergence on the global material balance, the distillation column is not a feasible one. The global material balance is assumed to be verified when

$$\sqrt{\sum_{i=1}^C \left[\sum_{k=1}^N \left(F_{ik} + \sum_{j=1}^R v_{ij} \zeta_{jk} \right) - P_i \right]^2} < \varepsilon_c. \quad (5)$$

The convergence of the recycle variable, R_F , is verified when

$$\left| \frac{R_F^n - R_F^{n-1}}{R_F^n} \right| < \varepsilon_R, \quad (6)$$

where ε_C and ε_R are appropriate values. The simulation process ends up with a feasible reactive distillation column, which obeys the global material balance to within 10^{-3} (ε_C in Eq. (5)). To avoid premature convergence on the torn variable without convergence on the global mass balance, the convergence criterion for the torn variable was set to a much lower value, 10^{-10} (ε_R in Eq. (6)).

3.2.8. Simulation results

The simulation method developed was validated by performing the simulation of the distillation column reported by Ciric and Gu (1994), corresponding to the best configuration obtained by these authors. For a better evaluation of the simulation algorithm proposed in the present work, the same column was simulated in the AspenPlus modular environment. Two other distillation columns obtained during the optimization using the MSIMPSA algorithm were simulated with the AspenPlus simulator. One was obtained including the constraints on the maximum values of vapor and liquid flow rates as proposed by Ciric and Gu (1994), while the other was obtained by relaxing these constraints.

The simulation of the distillation column reported by Ciric and Gu (1994) corresponds to the water and ethylene glycol composition and temperature profiles shown in Figs. 3 and 4. These figures show that the profiles obtained with the algorithm developed in this work are very close to the profiles obtained by Ciric and Gu, as expected since the column model is the same. In what concerns the liquid and vapor molar flows, column height, condenser and reboiler duties, the results obtained by these two methods are again the same, and very

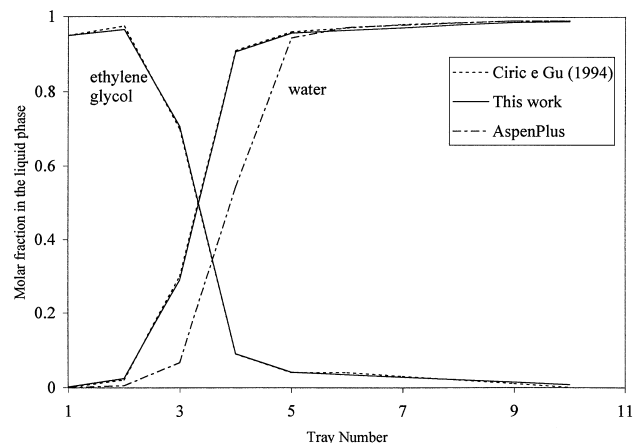


Fig. 3. Water composition and ethylene glycol profiles for the best solution obtained by Ciric and Gu (1994).

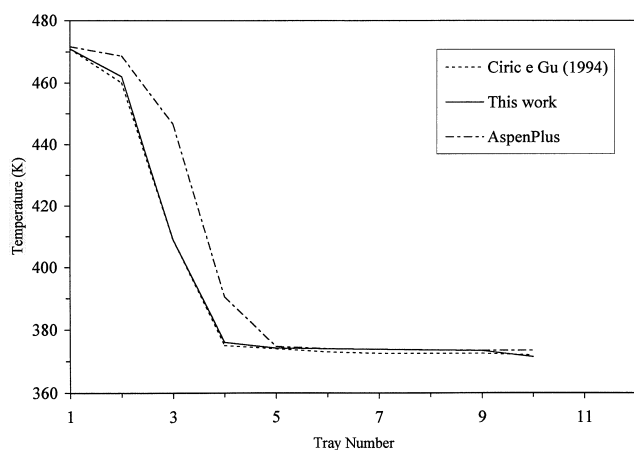


Fig. 4. Temperature profile for the best solution obtained by Ciric and Gu (1994).

close to those obtained with the AspenPlus simulator. However, at the bottom, the liquid and vapor molar flow rates obtained with AspenPlus differ from the other two simulators by 2%, and at the top, by 30%. The column diameters obtained by Ciric and Gu (1994), by the simulation method developed in this work and by the AspenPlus simulator are very close to each other, respectively, 1.30, 1.34 and 1.38 m.

The differences between the composition and temperature profiles obtained by the AspenPlus simulator and the other two simulators can be due not only to the different methods used to evaluate the physical properties, but also to the different assumptions made when developing the mathematical model for the column. The energy balance in the model proposed by Ciric and Gu (1994) and adopted in this work, Eq. (B.13), will only be valid with negligible enthalpies of the liquid streams and constant enthalpy of vaporization. The AspenPlus simulator most probably does not follow any of these assumptions, since the enthalpies of the liquid streams computed by this simulator are of the same order of magnitude as the enthalpies of the vapor streams, certainly not negligible. In the Ciric and Gu model, the energy balance used makes the vapor stream remain constant in the bottom trays where the reaction terms are null. This is the reason why the application of this model gives constant vapor and liquid flow rates for the first four trays, where there is no reaction. On the contrary the AspenPlus simulator gives rise to different flow rates, which changes the final simulation result. In spite of the different flow rates in the top trays, the profiles obtained with the different models are similar to each other, probably because in those trays there is reaction which is the main factor in establishing the tray compositions.

Figs. 5 and 6 show the profiles corresponding to a simulation obtained with the MSIMPISA algorithm with active constraints on the maximum molar flow

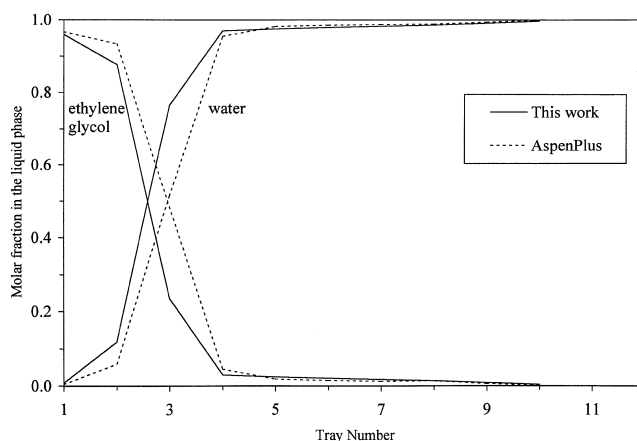


Fig. 5. Water and ethylene glycol composition profiles for a solution obtained with active constraints on the maximum molar flow rates.

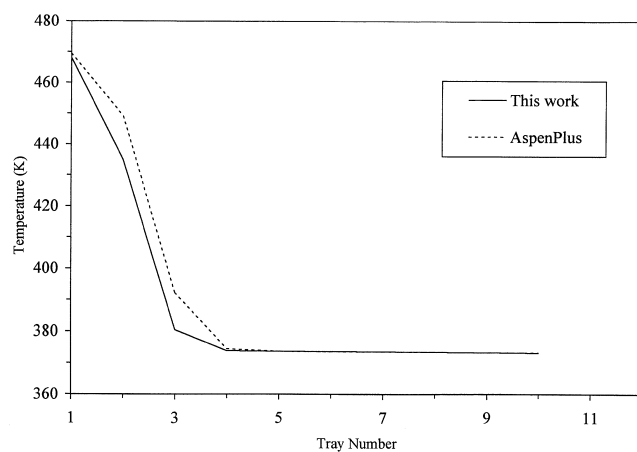


Fig. 6. Temperature profile for a solution obtained with active constraints on the maximum molar flow rates.

rates. It can be seen that the profiles obtained with the proposed simulation method and with the AspenPlus simulator are similar. Also, the column diameter is the same, 1.68 m.

The column specification obtained when the maximum liquid and vapor molar flow rates are relaxed is compared with the results obtained with the AspenPlus simulator in Figs. 7 and 8. It can be seen that the profiles are now nearly the same all over the column.

The profiles obtained with the proposed simulation algorithm and with the AspenPlus simulator are similar for the last two configurations. This can be due to the fact that in both configurations the reaction occurs in all trays.

In conclusion, the validation of the simulation method developed was performed by comparing the results obtained with those from the AspenPlus simulator, for three

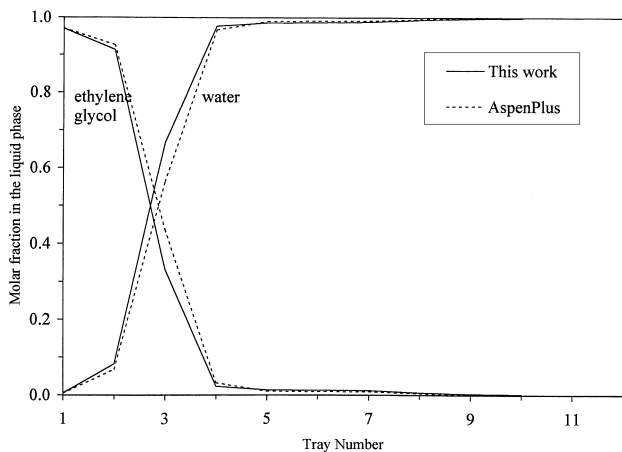


Fig. 7. Water and ethylene glycol composition profiles for a solution obtained without constraints on the maximum molar flow rates.

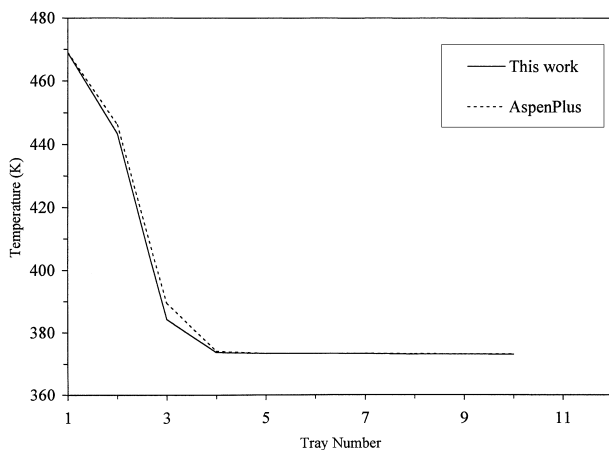


Fig. 8. Temperature profile for a solution obtained without constraints on the maximum molar flow rates.

different configurations of a reactive distillation column for the production of ethylene glycol. All column specifications correspond to feasible column designs. Even the configuration obtained with the MSIMPISA algorithm without taking into account constraints on the allowable liquid and vapor molar flow rates, which are 50% larger than the limits imposed by Ciric and Gu, corresponds to a feasible column. The AspenPlus simulator, with the same configuration, could also end up with a feasible column. This agrees with the heuristic rules given by Douglas (1988), which state that if there is neither flooding nor liquid entrainment there are no limits to the molar flow rates within the column. The only constraints stated by those rules are a maximum limit of 53 m in the column height, a minimum limit of 0.45 m in the diameter, and that the column diameter should be lower than 5% of the column height. None of these limits was violated in any of the above cases.

3.3. Optimization of the production of ethylene glycol via reactive distillation

3.3.1. Ideal vapor–liquid equilibrium

The synthesis of a non-equilibrium reactive distillation column for the production of ethylene glycol, as described above, was proposed and solved by Ciric and Gu (1994). These authors used a modified GBD algorithm (Geoffrion, 1972).

Ciric and Gu (1994) state that the GBD algorithm simply requires selecting an initial solution vector of the discrete variables, viz. the number of theoretical trays in the distillation column. In the GBD algorithm, a master problem selects the number of trays while a primal problem optimizes the continuous variables. For highly non-linear MINLPs, it is standard practice to solve a third optimization problem, between the master and the primal, to find a feasible set of continuous variables by minimizing the total constraint violation.

The MSIMPISA algorithm, developed for the solution of MINLP problems was applied to this example. With the MSIMPISA algorithm, the starting solution vectors of both continuous and discrete variables are randomly generated and correspond most probably to infeasible points. However, since this algorithm is an infeasible path method, it does not require neither an initial feasible point nor solving intermediate optimization problems for feasibility. For highly constrained and non-linear NLP or MINLP problems, a dynamic penalizing scheme is available for finding feasible solution sets, while maintaining convergence to the global optimum (Cardoso et al., 1997). This dynamic penalizing scheme roughly doubles the CPU time, but it was not needed in the present case.

The MSIMPISA algorithm adopts the stochastic scheme proposed by Dolan et al. (1989) for the generation of discrete configurations. Since this scheme only allows a one unit variation up or down to the next discrete value, large jumps in the discrete search space are not allowed from one iteration to the next, and this may weaken the optimization process. To allow larger variations, the number of trays in the column was represented by a binary expansion (Cardoso et al., 1997).

Firstly, the MSIMPISA algorithm was applied including the additional constraints on maximum molar flow rates as stated by Ciric (1995), and again an optimum configuration with 10 theoretical trays was obtained. The best solution found by the MSIMPISA algorithm has a total cost of 15.26×10^6 US\$ yr⁻¹, similar to the cost found by Ciric and Gu of 15.69×10^6 US\$ yr⁻¹. The solution vectors are however different, and the solution obtained with the MSIMPISA algorithm corresponds to active constraints on the maximum molar flow rates. The two solutions are compared in Table 2 and in Figs. 9 and 10. It can be seen that with the solution obtained in this work there is reaction in all trays and the feed is more

Table 2
Column specifications for the best configuration obtained, with constraints on the maximum molar flow rates (**this work**/Ciric and Gu (1994))^a

Tray	Feed		Liquid holdup (m ³)	Molar flow rate	
	Ethylene oxide (mol s ⁻¹)	Water (mol s ⁻¹)		Vapor (mol s ⁻¹)	Liquid (mol s ⁻¹)
1	0.00 /0.00	0.02 /0.00	0.30 /0.00	263.2 /168.2	270.4 /175.5
2	0.00 /0.00	0.00 /0.00	0.73 /0.00	263.2 /168.2	270.4 /175.5
3	0.00 /0.00	0.01 /0.00	1.20 /0.00	263.2 /168.2	270.4 /175.5
4	0.80 /0.00	0.17 /0.00	0.27 /0.00	264.2 /168.2	270.4 /175.5
5	1.00 /1.36	0.99 /0.00	0.78 /0.55	266.2 /170.4	271.0 /175.5
6	0.85 /1.32	0.61 /0.00	0.83 /0.48	268.0 /172.8	272.1 /177.5
7	0.90 /1.30	0.93 /0.00	0.98 /0.45	269.8 /175.2	273.3 /179.9
8	1.77 /1.38	1.89 /0.00	0.82 /0.37	272.9 /177.7	274.2 /182.3
9	1.43 /0.56	1.42 /0.00	0.75 /1.47	275.7 /180.3	275.2 /184.7
10	0.66 /2.24	1.20 /7.31	1.45 /0.01	277.6 /182.9	276.6 /188.5

^aColumn diameter = 1.7/1.3 m, column height = 9.7/12 m, $\beta = 0.973/0.958$, $Q_B = 10.5/6.7$ MW, $Q_C = 11.1/7.31$ MW.

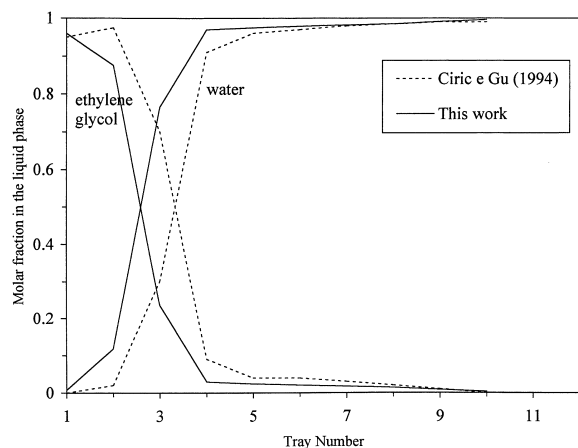


Fig. 9. Water and ethylene glycol composition profiles for the best solution obtained with active constraints on the maximum molar flow rates.

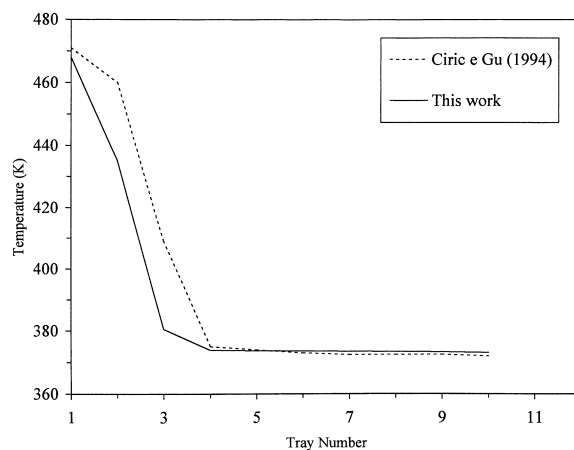


Fig. 10. Temperature profile for the best solution obtained with active constraints on the maximum molar flow rates.

distributed, mostly the water feed. Stein, Kienle, Esparta, Mohl and Gilles (1999), using the GAMS simulation environment with the CONOP non-linear optimizer, obtained an optimum solution which basically agrees with that of Ciric and Gu (1994), where the reaction and separation zones are distinct. The composition and temperature profiles for the solution obtained in this work and that of Ciric and Gu (1994) have however basically the same shape.

The constraints on liquid and vapor molar flow rates were thus relaxed, following the heuristic rules proposed by Douglas (1988), in an attempt to obtain better solutions while retaining feasible column designs. The MSIMPSA algorithm was applied to this relaxed MINLP problem. Starting from random points, 22 full MINLP optimizations were performed, and different

MINLP solutions were obtained (as the objective function is very flat), corresponding the best solution to 8 trays and a total cost of 15.12×10^6 US\$ yr⁻¹ (Cardoso et al., 1997).

The results were compared with those obtained with the MSGA algorithm (Salcedo, 1992), an MINLP adaptive random search method, starting from 14 different random points. The best result obtained corresponds to a column with 12 trays and 15.16×10^6 US\$ yr⁻¹, which is very close to the best cost obtained with the MSIMPSA algorithm. The average processing time spent in each run was about 0.8 s for the evaluation of each objective function, which roughly corresponds to 18 h with the MSIMPSA algorithm and 5 h with the MSGA algorithm. Although these times seem large, personal computers of the Pentium II (Intel) or G3-750 PPC

Table 3
Column specifications for the best solution obtained (ideal VLE)^a

Tray	Feed		Liquid holdup (m ³)	Molar flow rate	
	Ethylene oxide (mol s ⁻¹)	Water (mol s ⁻¹)		Vapor (mol s ⁻¹)	Liquid (mol s ⁻¹)
1	0.01	2.04	0.327	476.7	483.9
2	0.00	1.65	0.694	476.7	481.8
3	0.00	1.14	0.000	476.7	480.2
4	1.72	0.78	0.447	478.8	479.1
5	1.96	0.21	1.941	483.3	479.8
6	1.28	1.29	0.578	485.4	484.4
7	2.33	0.04	1.930	491.0	485.0

^aColumn diameter = 2.3 m, column height = 8.8 m, $\beta = 0.985$, $Q_B = 19.1$ MW, $Q_C = 19.6$ MW.

(IBM/Motorola) processor class can easily outperform the HP 730 workstation by a factor of 4.

Since the objective function is very flat, corresponding to different number of trays, systematic NLP searches were performed by directly enumerating the number of trays, and for each value of the discrete variable about 10 runs were performed. The best NLP solution corresponds to 7 trays and an objective function of 15.03×10^6 US\$ yr⁻¹, i.e. only 0.6% better than the best result obtained with the full MINLP formulation, which simultaneously optimizes the continuous and discrete variables. The best results obtained from the full MINLP search are within 1% of the best results obtained from the systematic NLP search. The results suggest that the MSIMPASA algorithm, when applied to the complete solution vector (continuous and discrete variables), obtains solutions similar to those obtained when applied only to the continuous variables (Cardoso et al., 1997). The results also suggest that the adaptive random search MSGA is capable of providing optimized solutions comparable to those previously reported.

The column specifications for the best solution obtained, with 7 trays and an objective function of 15.03×10^6 US\$ yr⁻¹, are given in Table 3 and the corresponding composition and temperature profiles are shown in Figs. 11 and 12.

The optimized designs found in this work have a highly distributed feed and reaction zones, and this might not be practical to implement. Thus, more practical designs may be obtained by constraining the feed distribution to only two streams, one for water and one for ethylene oxide, and the reaction zone to a single tray. Constraining the feed distribution and the reaction zone to a single tray is easily achieved within the proposed framework, since the reaction volumes and component feeds are decision variables, thus allowing comparison with the designs proposed by others (Okasinski & Doherty, 1998). It should be stated that the optimization problem becomes much easier for a single feed and reaction tray,

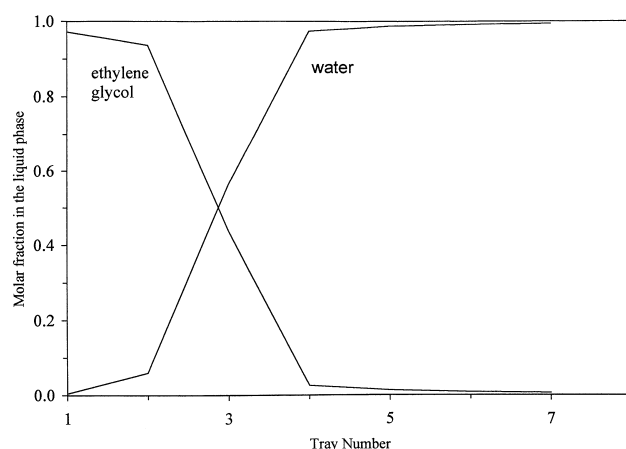


Fig. 11. Composition profiles for the best solution obtained (ideal VLE).

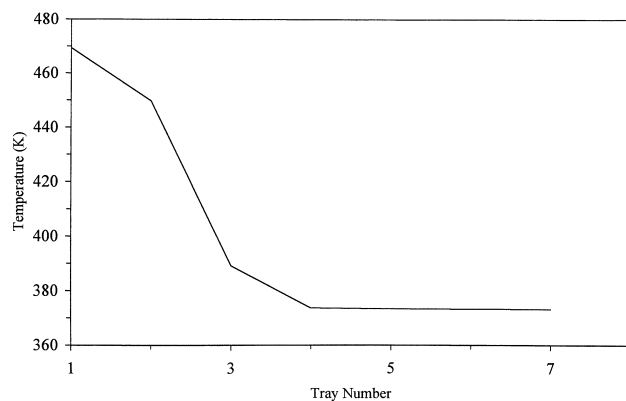


Fig. 12. Temperature profile for the best solution obtained (ideal VLE).

since the number of decision variables decreases substantially from a maximum of 61 (for 20 trays) down to 5. In this work, this was only performed considering non-ideal vapor-liquid equilibrium.

Typical trajectories for the best objective function values and the number of theoretical trays, for two full MINLP runs can be seen elsewhere (Cardoso et al., 1997), where it is shown that the MSIMPISA algorithm probes well the discrete search space.

Stein et al. (1999) have also solved this problem, but starting from a superstructure, where a reactive distillation column is one of the possible topologies. They have found that their best solution does correspond indeed to a reactive distillation column, but it is possible that this is simply a local optimal solution as the number of degrees of freedom was very large (439) and there was no guarantee that the global optimum configuration had been reached.

3.3.2. Non-ideal vapor–liquid equilibrium

Okasinski and Doherty (1998) have shown that the ideal equilibrium model used by Ciric and Gu (1994) is unrealistic, and propose that the Wilson model be used instead, since this gives vapor–liquid equilibrium curves much closer to those observed (Gmehling & Onken, 1977). They also propose that the column be operated at higher pressures (15 atm) to increase the reaction temperature and thus the reaction rate. These authors have further considered one single reaction, since water (W) in their design is highly in excess over ethylene oxide (EO), thus avoiding formation of the by-product diethylene glycol (DEG) in favor of ethylene glycol (EG). We have performed optimizations with a single reaction (three components), but very short columns (mostly 2-tray columns) were obtained with both the MSIMPISA and

MSGAs algorithms, using either ideal or non-ideal equilibrium. However, the composition profiles do not obey the requirement that water be in great excess over ethylene oxide, thus violating the hypothesis of a single reaction. To circumvent this problem, one of two approaches is possible: either imposing the constraint of excess water on every tray where reaction can take place, or using the Wilson model while taking both reactions into account. The second approach was chosen, since it does not constraint a priori the column to a suboptimal design. The Wilson constants for the systems DEG/EO, DEG/EG and DEG/W were obtained by fitting this model to equilibrium data generated by the UNIFAC method, and the results can be seen in Table 9.

Ten full MINLP optimizations were performed for both 1 and 15 atm allowing the reaction to proceed over several trays. The objective function is very flat, similar to what happened before with ideal VLE. Fig. 13 shows the composition profiles for the best solutions obtained, corresponding to 10 and 11 trays and an objective function of 15.10 and 15.12×10^6 US\$ yr⁻¹, respectively for 1 and 15 atm. Table 4 shows the corresponding temperature profiles, molar flow rates and reaction volumes. The main difference between the solutions at 1 and 15 atm is in the temperature profiles, and the main differences between the non-ideal and ideal VLE designs are in the molar flow rates and reboiler and condenser duties.

To better compare our results with the design proposed by Okasinski and Doherty (1998), which has a single feed and reaction zone, we have constrained the feed and reaction zone to a single (top) tray. For both

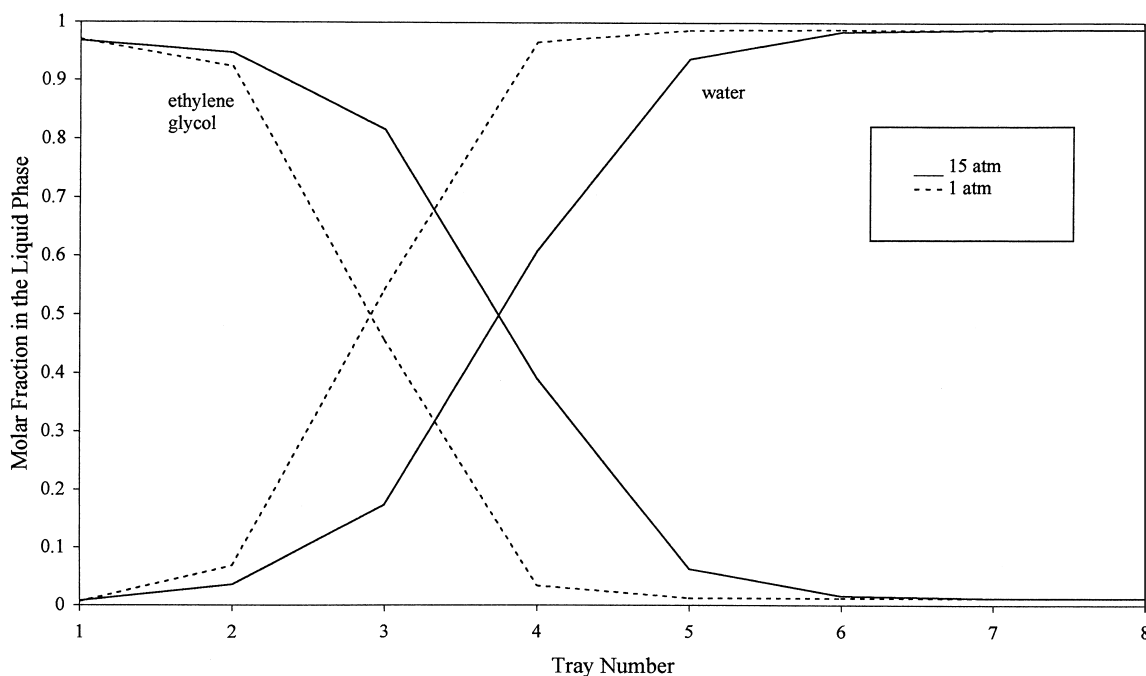


Fig. 13. Composition profiles for the best solution obtained (non-ideal VLE, distributed reaction zone).

Table 4
Column specification and temperature profiles for the best solution obtained (non-ideal VLE, distributed reaction zone): **pressure = 15 atm/**
pressure = 1 atm^a

Tray no.	Feed		Temperature (K)	Liquid holdup (m ³)	Molar flow	
	Ethylene oxide (mol s ⁻¹)	Water (mol s ⁻¹)			Vapor (mol s ⁻¹)	Liquid (mol s ⁻¹)
1	0.01/0.02	0.13/2.60	576.6/466.1	1.20/0.71	839.0/866.8	846.2/874.0
2	0.00/0.01	1.36/0.88	560.0/430.5	0.25/0.73	839.0/866.8	846.1/871.4
3	0.00/0.31	0.64/0.56	513.7/380.5	1.80/0.13	839.0/867.0	844.7/870.5
4	0.26/1.04	0.52/0.06	478.8/373.5	1.93/1.00	839.4/867.5	844.1/870.1
5	1.30/1.14	0.77/0.26	472.8/373.3	0.60/1.97	841.9/869.1	844.0/869.8
6	0.25/1.10	0.17/0.54	472.2/373.3	1.30/0.81	842.4/870.0	845.7/870.7
7	1.44/1.02	0.41/0.19	472.2/373.3	1.62/1.65	845.2/871.9	846.0/870.4
8	0.59/1.02	1.16/0.70	472.1/373.2	1.83/1.15	846.4/873.4	848.5/872.1
9	1.34/0.72	0.77/0.51	472.1/373.2	1.31/0.60	849.1/874.3	848.5/872.7
10	0.68/0.93	0.88/0.93	472.0/372.8	0.87/0.85	850.4/881.0	850.4/872.8
11	1.45/ —	0.45/ —	472.0/ —	1.24/ —	853.3/ —	850.9/ —

^aColumn diameter = 3.0/3.0 m, column height = 11.7/10.6 m, $\beta = 0.991/0.991$, $Q_B = 33.6/34.7$ MW, $Q_C = 34.1/35.2$ MW.

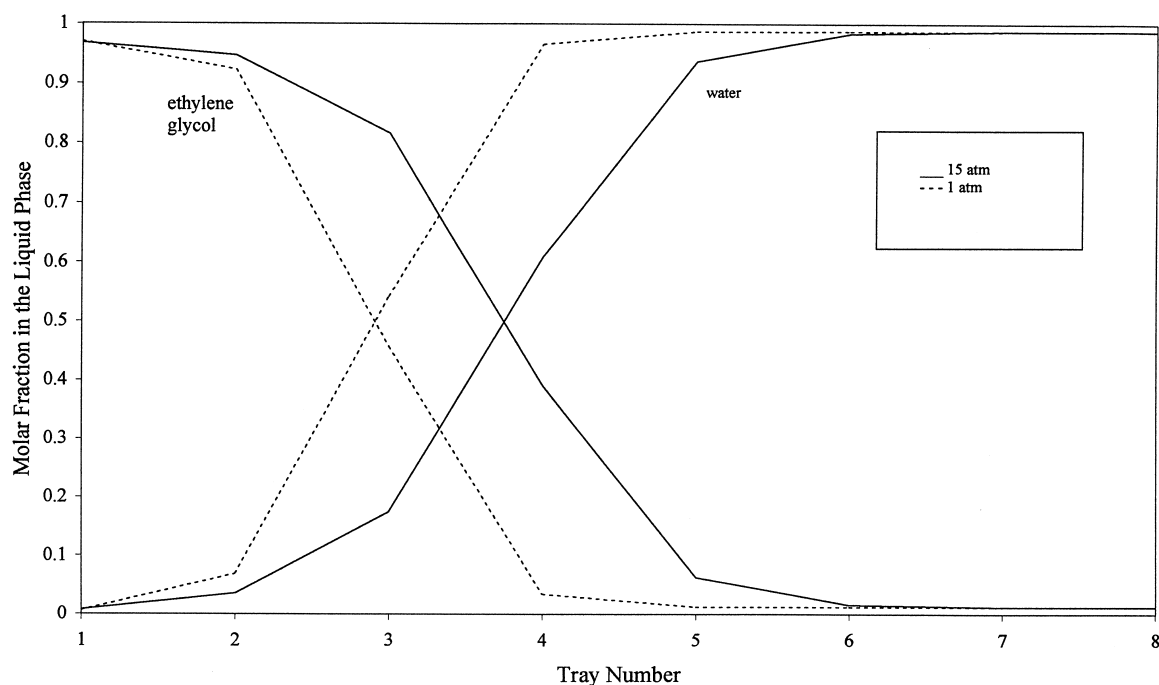


Fig. 14. Composition profile for the best solution obtained (non-ideal VLE, single reaction zone).

1 and 15 atm, the results show that the lower costs of 15.04 and 15.05×10^6 US\$ yr⁻¹ occur for a column with 7 and 8 trays, respectively at 1 and 15 atm. However, several feasible designs could be found from 5 to 17 trays with objective functions within 1% of the lowest cost, once more showing that the number of trays and column dimensions are not decisive variables. Fig. 14 shows the composition profiles for the best solutions obtained, and Table 5 shows the corresponding temperature profiles

and relevant computed variables. The water feed at the bottom of the column is not null, since this is the torn variable which is required for the entire simulation process. The optimum solutions for a single feed and reaction zone are marginally better (0.4%) than those for a distributed system, because the optimization problem is now much easier since the number of decision variables has decreased from up to 61 down to 5. Compared with the distributed feed designs, the molar volumes and the

Table 5
Column specification and temperature profiles for the best solution obtained (non-ideal VLE, distributed reaction zone):
pressure = 15 atm/pressure = 1 atm^a

Tray no.	Feed		Temperature (K)	Liquid holdup (m ³)	Molar flow	
	Ethylene oxide (mol s ⁻¹)	Water (mol s ⁻¹)			Vapor (mol s ⁻¹)	Liquid (mol s ⁻¹)
1	0.00/0.00	4.81/3.49	578.7/468.7	0.00/0.00	624.5/591.2	631.6/598.4
2	0.00/0.00	0.00/0.00	572.2/448.1	0.00/0.00	624.5/591.2	626.8/594.9
3	0.00/0.00	0.00/0.00	543.9/391.2	0.00/0.00	624.5/591.2	626.8/594.9
4	0.00/0.00	0.00/0.00	494.2/374.1	0.00/0.00	624.5/591.2	626.8/594.9
5	0.00/0.00	0.00/0.00	474.8/373.5	0.00/0.00	624.5/591.2	626.8/594.9
6	0.00/0.00	0.00/0.00	472.6/373.5	0.00/0.00	624.5/591.2	626.8/594.9
7	0.00/7.30	2.36/3.67	472.4/372.2	0.00/0.61	624.5/605.5	626.8/594.9
8	7.30/—	0.24/—	472.4/—	0.72/—	638.8/—	626.8/—

^aColumn diameter = 2.6/2.5 m, column height = 8.1/7.4 m, $\beta = 0.989/0.988$, $Q_B = 25.0/23.6$ MW, $Q_C = 25.6/24.2$ MW.

condenser and reboiler duties have decreased, and once again, the main difference between 1 and 15 atm is in the temperature profiles.

The reason why the results from the optimization are not significantly dependent on the number of trays, column dimensions and reboiler and condenser duties is directly related to the cost functions that make-up the objective function. A closer inspection of these cost terms shows that, at the optimum solutions, the reactant costs (EO and W) make-up for more than 99% of the total cost. However, this does not mean that any feasible design has a low cost, since feasible designs with a cost up to 40×10^6 US\$ yr⁻¹ can be easily obtained. Thus, with the available cost data, it may be concluded that while designing distillation columns for this reactive system may benefit from optimization, any optimized feasible column design will have approximately the same total annualized cost, irrespective of the column dimensions, distributed or single-tray feed and reaction zone.

4. Conclusions

Ciric and Gu (1994) propose an interesting technique for the synthesis of reactive distillation columns, which can be applied to generic situations where there is more than one chemical reaction, or when reaction equilibrium or constant molar flows cannot be assumed. With this column model they have built a MINLP problem. The solution of this problem yields the optimum number of trays, the optimal feed tray locations and the composition profiles. These authors solved the MINLP problem using a generalized Benders decomposition algorithm (Geoffrion, 1972), assuming ideal VLE.

In this work, we propose a new simulation/optimization model for the MINLP formulation of reactive distillation columns as per Ciric and Gu (1994), where the simulation algorithm is based on conventional distilla-

tion (Bastos, 1987) and the optimization is performed by stochastic algorithms, namely a simulated annealing-based MINLP algorithm (Cardoso et al., 1997) and an adaptive random search MINLP algorithm (Salcedo, 1992). The simulation starts with an initial estimate of one molar feed flow rate not specified by the decision vector, viz. a torn variable. An estimate of the initial composition profile in the column is next obtained, which is further improved by a relaxation method. The material balance equations are then solved with the Newton–Raphson method, and a new composition profile is computed. The torn variable is re-evaluated and the equations describing the reactive distillation process are again solved. The algorithm ends up when the global material balance to the column is obeyed, after convergence on the torn variable, or when a non-plausible column is obtained. The problem solved is fairly large and highly non-linear, with a maximum (for a 20 tray column) of 61 degrees of freedom.

Optimizations were performed with both ideal and non-ideal VLE, and in this last case at 1 and 15 atm, for uncatalyzed reactions. For non-ideal VLE, optimizations were also performed by constraining the reaction zone to a single (top) tray. The results show that, irrespective of the VLE model and operating pressures, the objective function is very flat, with similar values at the optimum designs. This is also true if the feed and reaction zone is constrained to a single (top) tray. It can be concluded that, for this system, the number of theoretical stages is not an important decision variable, and optimum columns may be designed by fixing the number of stages (anywhere between 5 and 17) and simply solving the resulting NLP subproblem.

The results show that the proposed simulation/optimization algorithms are capable of providing solutions which are very close to the global optimum, and thus constitute viable methods for the design of reactive distillation columns. Further improvements include the use of

a more general energy balance and heterogeneous reactive mixtures. The stochastic algorithms may also prove useful in studying the influence of the localization of the reaction zone in reactive distillation processes.

Acknowledgements

This work was partially supported by FCT (Portuguese Foundation for Science and Technology) under contract PRAXIS/3/3.1/CEG /22641/95, employing the computational facilities of Instituto de Sistemas e Robótica (ISR) — Porto. The authors thank Dr. J. Bastos for providing crucial parts of the code needed to simulate the distillation process.

Appendix A

Physical, reaction and cost data are given in Tables 6–9.

Appendix B. Mathematical problem formulation

B.1. Objective function and cost terms

$$\text{FOB}_j = \min \left\{ \sum_{i=1}^C c_i \sum_{k=1}^N F_{ik} + c_H Q_B + c_W Q_C + A_F (C_{cs} + C_{ci} + C_r + C_c) \right\}. \quad (\text{B.1})$$

Here, c_i is the cost of raw material i , F_{ik} is the feed rate of material i to tray k , c_H is the cost of steam, c_W is the cost of cooling water, and Q_B and Q_C correspond to reboiler and condenser duties. A_F is an annualizing factor; C_{cs} , C_{ci} , C_r and C_c are the installed costs of the

Table 6
Reaction data^a

Reaction	Rate (mol m ⁻³ s ⁻¹)	ΔH (J mol ⁻¹)
(R1)	$3.15 \times 10^{15} \exp(-9547/T)x_1x_2$	-80.0×10^3
(R2)	$6.3 \times 10^{15} \exp(-9547/T)x_1x_3$	-13.1×10^3

^a T — temperature (K).

Reaction (R1) — Production of ethylene glycol from ethylene oxide and water.

Reaction (R2) — Production of diethylene glycol from ethylene glycol and ethylene oxide.

Table 7
Vapor–liquid equilibrium constant, K , at 1 atm^a

Component	K (dimensionless)
Ethylene oxide	$71.9 \exp\{5.720[(T - 469)/(T - 35.9)]\}$
Water	$221.2 \exp\{6.310[(T - 647)/(T - 52.9)]\}$
Ethylene glycol	$77.0 \exp\{9.940[(T - 645)/(T - 71.4)]\}$
Diethylene glycol	$47.0 \exp\{10.42[(T - 681)/(T - 80.6)]\}$

^a T — temperature (K).

Table 8
Cost data

Ethylene oxide cost	43.7×10^{-3} US\$ mol ⁻¹
Water cost	21.9×10^{-3} US\$ mol ⁻¹
c_{SH}	222 US\$ yr ⁻¹
c_T	15.7 US\$ yr ⁻¹
c_R	146.8×10^{-3} US\$ W ⁻¹ yr ⁻¹
c_C	24.5×10^{-3} US\$ W ⁻¹ yr ⁻¹
c_0	10,000 US\$ yr ⁻¹

Table 9
Thermodynamic data for the non-ideal VLE case

Component	Ethylene oxide	Water	Ethylene glycol	Diethylene glycol
Normal boiling point (K)	283.85	373.15	470.4	518.0
Antoine coeff.				
A_1	21.3066	23.2256	25.1431	34.4262
A_2	-2428.2	-3835.18	-6022.18	-16,224.92
A_3	-35.388	-45.343	-28.25	190.015
Wilson coeff. (cal mol ⁻¹)				
EO	—	124.965	-79.471	157.874
W	1905.77	—	1266.0109	923.33
EG	635.823	-1265.7398	—	-112.337
DEG	220.233	-180.210	856.192	—
Molar volume (ml mol ⁻¹)	49.909	18.07	55.92	94.78

column shell, trays, reboiler, and condenser. The column investment costs is calculated by (Douglas, 1988)

$$C_{cs} = 0.3639(M\&S)D^{1.066}H^{0.802}(2.18 + F_c), \quad (B.2)$$

$$C_{ci} = \sum_{k=1}^N 0.0168(M\&S)D^{1.55}H_k F'_c. \quad (B.3)$$

Here, M&S is the Marshall and Swift Index published periodically by the Chemical Engineering Journal, D is the column diameter, H is the height of the column, F_c and F'_c are construction factors and H_k is the height of tray k . Eq. (B.2) is simplified by assuming $D^{1.066} \approx D$ (Ciric & Gu, 1994). The reboiler and condenser investment costs are evaluated by

$$C_r = cr_1 + cr_2 Q_B, \quad (B.4)$$

$$C_c = cc_1 + cc_2 Q_C. \quad (B.5)$$

The height of the tower is evaluated by

$$H = H_0 + \sum_{k=1}^N H_k, \quad (B.6)$$

where H_0 is a fixed extra column height corresponding to the free space below the bottom tray and above the top tray. The heights H_k are evaluated by adding the minimum tray spacing, H_{\min} , to the height of liquid in tray k , corresponding to volume W_k :

$$H_k = H_{\min} + 1.27 \frac{W_k}{D^2}. \quad (B.7)$$

Ciric and Gu (1994) set H_0 and H_{\min} respectively to 3.0 and 0.61 m. Substitution of these expressions into Eq. (B.1), after some algebraic simplification, provides

$$\begin{aligned} \text{FOB}_j = \min \left\{ c_0 + \sum_{i=1}^c c_i \sum_{k=1}^N F_{ik} + c_R Q_B + c_C Q_C + c_T D^{1.55} \right. \\ \left. \times \sum_{k=1}^N \left(0.61 + 1.27 \frac{W_k}{D^2} \right) \right. \\ \left. + c_{SH} D \left(H_0 + \sum_{k=1}^N \left(0.61 + 1.27 \frac{W_k}{D^2} \right) \right)^{0.802} \right\}, \end{aligned} \quad (B.8)$$

where c_0 , c_i , c_R , c_C , c_T and c_{SH} correspond to cost parameters.

Ciric and Gu (1994) developed a reactive distillation column model based on the following assumptions: the vapor and liquid phases are in equilibrium on each tray; no reaction occurs in the vapor phase; the liquid phase is always homogeneous; the enthalpy of the liquid streams is negligible; the enthalpy of vaporization is constant; and

both condenser and reboiler are total. They also made the assumption that the temperature dependence of the reaction rates can be expressed in an Arrhenius form. Stein et al. (1999) have also adopted this model, but allowing for temperature- and concentration-dependent molar enthalpies.

B.2. Column model

The reactive distillation model, proposed by Ciric and Gu (1994), is given by the following equations:

B.2.1. Material, energy and stoichiometric balances

Material balance over the bottom tray:

$$F_{i1} - L_1 x_{i1} (1 - \beta) + L_2 x_{i2} - V_1 K_{i1} x_{i1} + \sum_{j=1}^R v_{ij} \zeta_{j1} = 0, \quad i = 1, \dots, C. \quad (B.9)$$

Material balance over tray k :

$$F_{ik} + V_{k-1} K_{ik-1} x_{ik-1} + L_{k+1} x_{ik+1} - L_k x_{ik} - V_k K_{ik} x_{ik} + \sum_{j=1}^R v_{ij} \zeta_{jk} = 0, \quad k = 2, \dots, N, \quad i = 1, \dots, C. \quad (B.10)$$

Stoichiometric equations:

$$\sum_{i=1}^c x_{ik} - 1 = 0, \quad k = 1, \dots, N, \quad (B.11)$$

$$\sum_{i=1}^c K_{ik} x_{ik} - 1 = 0, \quad k = 1, \dots, N. \quad (B.12)$$

Energy balance over tray k :

$$\lambda V_{k-1} - \lambda V_k - \sum_{j=1}^R \Delta H_j \zeta_{jk} = 0, \quad k = 1, \dots, N. \quad (B.13)$$

Material balance over the reboiler:

$$B_i = (1 - \beta) L_1 x_{i1}, \quad i = 1, \dots, C. \quad (B.14)$$

Overall balance of component i :

$$x d_i D_{\text{ist}} + B_i = P_i, \quad i = 1, \dots, C, \quad (B.15)$$

where F_{ik} is the flow rate of component i onto tray k , V_k is the vapor flow rate off tray k , ζ_{ik} is the vapor–liquid partition coefficient for component i on tray k , x_{ik} is the mole fraction of component i on liquid phase off tray k , L_k is the liquid flow rate off tray k , v_{ij} is the stoichiometric coefficient of component i in reaction j , ζ_{jk} is the extent of reaction j on tray k , B_i is the flow rate of component i off the bottom of the column and P_i is the production rate of component i .

The distillate molar flow, D_{ist} , is calculated from the difference between the vapor flow off the top tray, V_N , and the liquid flow onto it, L_{N+1} :

$$D_{\text{ist}} = V_N - L_{N+1}. \quad (\text{B.16})$$

Since the condenser is total, these three flows (D_{ist} , V_N and L_{N+1}) have the same composition:

$$x_{iN+1} = x_{di}, \quad i = 1, \dots, C, \quad (\text{B.17})$$

$$x_{di} = K_{iN} x_{iN}, \quad i = 1, \dots, C. \quad (\text{B.18})$$

The molar flow rate off the bottom, V_0 , is given by βL_1 , where β is the boil-up fraction of L_1 vaporized in the reboiler:

$$\beta = \frac{V_0}{L_1}. \quad (\text{B.19})$$

B.2.2. Kinetics and thermodynamic relationships

The extent of reactions (ξ_{jk}) and the vapor-liquid partition coefficients (K_{ik}) are computed for component i on each tray k , by

$$\xi_{jk} = W_k f_j(x_{ik}, T_k), \quad k = 1, \dots, N, \quad j = 1, \dots, R, \\ i = 1, \dots, C, \quad (\text{B.20})$$

$$K_{ik} = K_{ik}(x_{ik}, T_k), \quad k = 1, \dots, N, \quad i = 1, \dots, C. \quad (\text{B.21})$$

Here W_k and T_k are the liquid holdup and the temperature of tray k .

B.2.3. Reboiler and condenser duties

The reboiler (Q_B) and condenser (Q_C) duties can be respectively found from

$$Q_B = \beta \lambda L_1, \quad (\text{B.22})$$

$$Q_C = \lambda V_N. \quad (\text{B.23})$$

Q_B is computed as the energy required to vaporize a fraction β of the liquid off the bottom tray, and Q_C is computed as the energy required to completely condense the vapor flow rate off the top tray.

B.2.4. Column diameter

The column design requires the evaluation of the diameter, D , which is computed for the conditions at the bottom of the column from the following relationship (Douglas, 1988; Ciric & Gu, 1994):

$$D^4 = C_D \beta^2 L_1^2, \quad (\text{B.24})$$

where C_D is a constant evaluated knowing the molecular weight of the gas, the bubble point of the gas and the column pressure.

Appendix C. Simulation model

C.1. Relaxation method

The relaxation method used is based on the method described by Bastos (1987), where the composition profile is improved by the following relationship:

$$x_{ik}^{n+1} = x_{ik}^n + \alpha [F_{ik} + V_{k-1} K_{ik-1} x_{ik-1}^n + L_{k+1} x_{ik+1}^n \\ - L_k x_{ik}^n - V_k K_{ik} x_{ik}^n + \sum_{j=1}^R v_{ij} \xi_{jk}], \\ k = 1, \dots, N, \quad i = 1, \dots, C, \quad (\text{C.1})$$

where α is the relaxation factor and n is the iteration number. Similar relaxation schemes are adopted by Lee and Dudukovic (1998) for the first 20 iterations. The use of a relaxation method to estimate liquid compositions near zero can generate large errors, involving not only this composition but also the composition of the other components. When this happens, problem-specific strategies are needed, such as those discussed later in the paper. With the new composition profile, the temperature profile and flow rates are computed as described before.

C.2. The Newton-Raphson method

The application of this method was based on the algorithm proposed by Bastos (1987), considering that the chemical reaction may be distributed over several column trays. For this process the material balance equations become

$$\Delta M_{i1} = F_{i1} - L_1 x_{i1} (1 - \beta) + L_2 x_{i2} - V_1 K_{i1} x_{i1} \\ + \sum_{j=1}^R v_{ij} \xi_{j1}, \quad i = 1, \dots, C, \quad (\text{C.2})$$

$$\Delta M_{ik} = F_{ik} + V_{k-1} K_{ik-1} x_{ik-1} + L_{k+1} x_{ik+1} \\ - L_k x_{ik} - V_k K_{ik} x_{ik} + \sum_{j=1}^R v_{ij} \xi_{jk}, \\ k = 2, \dots, N, \quad i = 1, \dots, C. \quad (\text{C.3})$$

The application of the Newton-Raphson method to this non-linear system can be written as

$$\mathbf{x}^{n+1} = \mathbf{x}^n + \Delta \mathbf{x}^n, \quad (\text{C.4})$$

where

$$\Delta \mathbf{x} = - \left[\frac{\partial \Delta M}{\partial \mathbf{x}} \right]^{-1} \Delta M \quad (\text{C.5})$$

and $[\partial \Delta M / \partial \mathbf{x}]$ is the Jacobian matrix of the system of equations. If the liquid-vapor equilibrium constant is not

dependent on the composition, the non-null elements of the Jacobian matrix are

$$\frac{\partial M_{ik}}{\partial x_{mk-1}} = V_{k-1} K_{ik-1} \delta_{im}, \quad k = 2, \dots, N, \quad i, m = 1, \dots, C \quad (C.6)$$

$$\frac{\partial M_{i1}}{\partial x_{m1}} = [-L_1(1 - \beta) - V_1 K_{i1}] \delta_{im} + \sum_{j=1}^R v_{ij} \frac{\partial \xi_{i1}}{\partial x_{m1}}, \quad i, m = 1, \dots, C, \quad (C.7)$$

$$\frac{\partial M_{ik}}{\partial x_{mk}} = (-L_k - V_k K_{ik}) \delta_{im} + \sum_{j=1}^R v_{ij} \frac{\partial \xi_{ik}}{\partial x_{mk}}, \quad k = 2, \dots, N - 1, \quad i, m = 1, \dots, C, \quad (C.8)$$

$$\frac{\partial M_{iN}}{\partial x_{mN}} = (-L_k) \delta_{im} + \sum_{j=1}^R v_{ij} \frac{\partial \xi_{iN}}{\partial x_{mN}}, \quad i, m = 1, \dots, C, \quad (C.9)$$

$$\frac{\partial M_{ik}}{\partial x_{mk+1}} = L_{k+1} \delta_{im}, \quad k = 1, \dots, N - 1, \quad i, m = 1, \dots, C, \quad (C.10)$$

where

$$\delta_{im} = 0, \text{ if } i \neq m, \quad \delta_{im} = 1, \text{ if } i = m.$$

Since the equations for the k stage contain variables that belong to the $k - 1$, k and $k + 1$ stages only, the Jacobian matrix is block tridiagonal, where each block is a square matrix of dimension $C \times C$. The Jacobian matrix has the following form:

B_1	C_1	0	0	0	...	0	0	0	0
A_2	B_2	C_2	0	0	...	0	0	0	0
0	A_3	B_3	C_3	0	...	0	0	0	0
0	0	0	0	0	0
0	0	0	0	0	0
0	0	A_{N-2}	B_{N-2}	C_{N-2}	0
0	0	0	A_{N-1}	B_{N-1}	C_{N-1}
0	0	0	0	A_N	B_N

Matrices A_k , B_k and C_k contain the partial derivatives of the equations describing the k th stage with respect to the liquid composition of trays $k - 1$, k and $k + 1$, and are computed with Eqs. (C.6)–(C.10). The system of equations is solved by Gaussian elimination in each matrix formed by the B_k , C_k , A_{k+1} and B_{k+1} submatrices, starting with $k = 1$ and B_1 , C_1 , A_2 and B_2 are then evaluated. The procedure is repeated for $k = 2, \dots, N - 1$, but only C_k , A_{k+1} and B_{k+1} must be evaluated since B_k has been evaluated in the previous step. Since negative values for the composition can be obtained with the Newton–Raphson method, a relaxation factor, η_k ,

is defined such that compositions are always positive. Eq. (C.4) is now written as

$$x_{ik}^{n+1} = x_{ik}^n + \Delta x_{ik} \eta_k, \quad k = 1, \dots, N, \quad i = 1, \dots, C, \quad (C.11)$$

where η_k takes values between zero and one. The compositions obtained are normalized such that Eq. (B.11) is obeyed. With the composition profile the new temperature and flow rate profiles are evaluated. All the calculations are then repeated until convergence of the Newton–Raphson method.

The Newton–Raphson method performs better with an appropriate starting guess, and this estimate can be improved with the relaxation method described by Eq. (C.1). Due to the specificity of the problem, a suitable value for the relaxation factor, $\alpha = 10^{-3}$, was obtained by trial and error. This value gives good convergence in the simulation process, and produces values with physical significance for all variables.

References

- Abufares, A. A., & Douglas, P. L. (1995). Mathematical modelling and simulation of the MTBE catalytic distillation process using speedup and AspenPlus. *Transactions of the Institution of Chemical Engineers*, 73, 3.
- Backhaus, A. A. (1921a). Continuous process for the manufacture of esters, US Patent No. 1400, 849.
- Backhaus, A. A. (1921b). Apparatus for the manufacture of esters, US Patent No. 1400, 850.
- Backhaus, A. A. (1921c). Apparatus for the production of esters, US Patent No. 1400, 851.
- Backhaus, A. A. (1922a). Apparatus for producing high-grade esters, US Patent No. 1403, 224.
- Backhaus, A. A. (1922b). Apparatus for esterification, US Patent No. 1403, 225.
- Backhaus, A. A. (1922c). Apparatus for the manufacture of esters, US Patent No. 1425, 624.
- Backhaus, A. A. (1922d). Process for the manufacture of esters, US Patent No. 1425, 625.
- Backhaus, A. A. (1922e). Methods for the production of ester-condensation products, US Patent No. 1425, 626.
- Backhaus, A. A. (1923a). Process of producing high-grade esters, US Patent No. 1454, 462.
- Backhaus, A. A. (1923b). Process of esterification, US Patent No. 1454, 463.

- Barbosa, D., & Doherty, M. F. (1988a). Design and minimum-reflux calculations for single-feed multicomponent reactive distillation columns. *Chemical Engineering Science*, 43(7), 1537.
- Barbosa, D., & Doherty, M. F. (1988b). Design and minimum-reflux calculations for double-feed multicomponent reactive distillation columns. *Chemical Engineering Science*, 43(7), 2377.
- Bastos, J. (1987). Modeling extractive distillation processes. Ph.D. thesis, Universidade do Porto (in Portuguese).
- Biegler, L. T., Grossmann, I. E., & Westerberg, A. W. (1997). *Systematic methods of chemical process design*. New Jersey: Prentice-Hall PTR.
- Buzad, G., & Doherty, M. F. (1995). New tools for the design of kinetically controlled reactive distillation columns for ternary mixtures. *Computers & Chemical Engineering*, 19(4), 395.
- Cardoso, M. F. (1998). Searching for the global optimum — a new strategy for the global optimization of MINLP problems, PhD thesis, Universidade do Porto (in Portuguese).
- Cardoso, M. F., Salcedo, R. L., & de Azevedo, S. F. (1994). Nonequilibrium simulated annealing: A faster approach to combinatorial minimization. *Industrial and Engineering Chemistry Research*, 33(8), 1908–1912.
- Cardoso, M. F., Salcedo, R. L., & de Azevedo, S. F. (1996). The simplex-simulated annealing approach to continuous nonlinear optimization. *Computers & Chemical Engineering*, 20(9), 1065–1080.
- Cardoso, M. F., Salcedo, R. L., de Azevedo, S. F., & Barbosa, D. (1997). A simulated annealing approach to the solution of MINLP problems. *Computers & Chemical Engineering*, 21(12), 1349–1364.
- Chang, Y. A., & Seader, J. D. (1988). Simulation of continuous reactive distillation by a homotopy-continuation method. *Computers & Chemical Engineering*, 12(12), 1243.
- Ciric, A. R. 1995. Personal communication, March 14.
- Ciric, A. R., & Gu, D. (1994). Synthesis of nonequilibrium reactive distillation processes by MINLP optimization. *AIChE Journal*, 40(9), 1479.
- Doherty, M. F., & Buzad, G. (1992). Reactive distillation by design. *Transactions of the Institution of Chemical Engineers*, 70, 448.
- Dolan, W. B., Cummings, P. T., & Levan, M. D. (1989). Process optimization via simulated annealing: Application to network design. *AIChE Journal*, 35(5), 725.
- Douglas, J.M. (1988). *Conceptual design of chemical processes*. New York: McGraw-Hill.
- Geoffrion, A. M. (1972). Generalized benders decomposition. *Journal of Optimization Theory and its Applications*, 10(4), 237.
- Gmehling, J., & Onken, U. (1977). *Vapor-liquid equilibrium data collection, aqueous-organic systems*. DECHEMA chem. data series, DECHEMA, Frankfurt/Main, Germany.
- Grossmann, I. E., & Daichendt, M. M. (1994). New trends in optimization approaches to process synthesis. In En Sup Yoon, *Proceedings of PSEi94, Fifth international symposium on process systems engineering*, Korean Institute of Chemical Engineers, Kyongju, Korea (p. 95).
- Hunek, J., Foldes, P., & Sawinsky, J. (1979). Methods for calculating reactive distillation. *International Chemical Engineering*, 19(2), 248.
- Huss, R. S., Chen, F., Malone, M. F., & Doherty, M. F. (1999). Computer aided tools for the design of reactive distillation systems. *Computers & Chemical Engineering*, (Suppl.), 23, S955.
- Jimoh, M., Arellano-Garcia, H., Bock, H., & Wozny, G. (1999). Experimental validation of a dynamic simulation model for the process integration of reaction and distillation using a purpose-built pilot plant PRES'99. In F. Friedler, & J. Klemes, *Proceedings of the second conference on process integration, modelling and optimization for energy saving and pollution reduction* (p. 361).
- Kirkpatrick, S., Gellatt, C. D., & Vecchi, M. P. (1983). Optimization by simulated annealing. *Science*, 220, 671.
- Ledet, W. P. & Himmelbleau, D. M. (1970). Decomposition procedures for the solving of large scale systems. In T. B. Drew, G. K. Cokelet, J. W. Hoopes Jr., & T. Vermewen, *Advances in Chemical Engineering*, vol. 8 (pp. 185–254), New York: Academic Press.
- Lee, Jin-Ho, & Dudukovic, M. P. (1998). A comparison of the equilibrium and nonequilibrium models for a multicomponent reactive distillation column. *Computers & Chemical Engineering*, 23, 159.
- Metropolis, N., Rosenbluth, A., Rosenbluth, M., Teller, A., & Teller, E. (1953). Equation of state calculations by fast computing machines. *Journal of Chemical Physics*, 21, 1087.
- Murthy, A. K. S. (1984). Simulation of distillation column reactors. *Proceedings of summer comput. simulation conference*, vol. 1 (p. 630).
- Nelder, J. A., & Mead, R. (1965). A simplex method for function minimization. *Computer Journal*, 7, 308.
- Okasinski, M. J., & Doherty, M. F. (1998). Design methods for kinetically controlled, staged reactive distillation columns. *Industrial and Engineering Chemistry Research*, 37(7), 2821.
- Pekkanen, M. (1995). A Local optimization method for the design of reactive distillation. *Computers & Chemical Engineering* (Suppl.), 19, S235.
- Press, W. H., & Teukolsky, S. A. (1991). Simulated annealing over continuous spaces. *Computational Physics*, 5(4), 426.
- Salcedo, R. L. (1992). Solving nonconvex nonlinear programming and mixed-integer nonlinear programming problems with adaptive random search. *Industrial and Engineering Chemistry Research*, 31(1), 262.
- Schenk, M., Gani, R., Bogle, I. D. L., & Pistikopoulos, E. N. (1999). A hybrid approach for reactive separation systems. *Computers & Chemical Engineering*, (Suppl.), 23, S419.
- Schoen, F. (1991). Stochastic techniques for global optimization: A survey of recent advances. *Journal of Global Optimization*, 1, 207.
- Stein, E., Kienle, A., Esparta, A. R. J., Mohl, K. D., & Gilles, E. D. (1999). Optimization of a reactor network for ethylene glycol synthesis — an algorithm approach. *Computers & Chemical Engineering* (Suppl.), 23, S903.
- Suzuki, I., Yagi, H., Kamatsu, H., & Hirata, M. (1971). Calculation of multicomponent distillation accompanied by a chemical reaction. *Journal of Chemical Engineering of Japan*, 4(1), 26.
- Venkataraman, S., Chan, W. K., & Boston, J. (1990). Reactive distillation using AspenPlus. *Chemical Engineering Progress*, 86(8), 45.